

Measurement of the $B^+ \rightarrow p\bar{p}K^+$ Branching Fraction and Study of the Decay Dynamics

- B. Aubert,¹ R. Barate,¹ D. Boutigny,¹ F. Couderc,¹ Y. Karyotakis,¹ J. P. Lees,¹ V. Poireau,¹ V. Tisserand,¹
A. Zghiche,¹ E. Grauges,² A. Palano,³ M. Pappagallo,³ A. Pompili,³ J. C. Chen,⁴ N. D. Qi,⁴ G. Rong,⁴ P. Wang,⁴
Y. S. Zhu,⁴ G. Eigen,⁵ I. Ofte,⁵ B. Stugu,⁵ G. S. Abrams,⁶ M. Battaglia,⁶ A. B. Breon,⁶ D. N. Brown,⁶
J. Button-Shafer,⁶ R. N. Cahn,⁶ E. Charles,⁶ C. T. Day,⁶ M. S. Gill,⁶ A. V. Gritsan,⁶ Y. Groysman,⁶
R. G. Jacobsen,⁶ R. W. Kadel,⁶ J. Kadyk,⁶ L. T. Kerth,⁶ Yu. G. Kolomensky,⁶ G. Kukartsev,⁶ G. Lynch,⁶
L. M. Mir,⁶ P. J. Oddone,⁶ T. J. Orimoto,⁶ M. Pripstein,⁶ N. A. Roe,⁶ M. T. Ronan,⁶ W. A. Wenzel,⁶ M. Barrett,⁷
K. E. Ford,⁷ T. J. Harrison,⁷ A. J. Hart,⁷ C. M. Hawkes,⁷ S. E. Morgan,⁷ A. T. Watson,⁷ M. Fritsch,⁸ K. Goetzen,⁸
T. Held,⁸ H. Koch,⁸ B. Lewandowski,⁸ M. Pelizaeus,⁸ K. Peters,⁸ T. Schroeder,⁸ M. Steinke,⁸ J. T. Boyd,⁹
J. P. Burke,⁹ N. Chevalier,⁹ W. N. Cottingham,⁹ M. P. Kelly,⁹ T. Cuhadar-Donszelmann,¹⁰ B. G. Fulsom,¹⁰
C. Hearty,¹⁰ N. S. Knecht,¹⁰ T. S. Mattison,¹⁰ J. A. McKenna,¹⁰ A. Khan,¹¹ P. Kyberd,¹¹ M. Saleem,¹¹
L. Teodorescu,¹¹ A. E. Blinov,¹² V. E. Blinov,¹² A. D. Bukin,¹² V. P. Druzhinin,¹² V. B. Golubev,¹²
E. A. Kravchenko,¹² A. P. Onuchin,¹² S. I. Serednyakov,¹² Yu. I. Skovpen,¹² E. P. Solodov,¹² A. N. Yushkov,¹²
D. Best,¹³ M. Bondioli,¹³ M. Bruinsma,¹³ M. Chao,¹³ I. Eschrich,¹³ D. Kirkby,¹³ A. J. Lankford,¹³
M. Mandelkern,¹³ R. K. Mommsen,¹³ W. Roethel,¹³ D. P. Stoker,¹³ C. Buchanan,¹⁴ B. L. Hartfiel,¹⁴
A. J. R. Weinstein,¹⁴ S. D. Foulkes,¹⁵ J. W. Gary,¹⁵ O. Long,¹⁵ B. C. Shen,¹⁵ K. Wang,¹⁵ L. Zhang,¹⁵ D. del Re,¹⁶
H. K. Hadavand,¹⁶ E. J. Hill,¹⁶ D. B. MacFarlane,¹⁶ H. P. Paar,¹⁶ S. Rahatloo,¹⁶ V. Sharma,¹⁶ J. W. Berryhill,¹⁷
C. Campagnari,¹⁷ A. Cunha,¹⁷ B. Dahmes,¹⁷ T. M. Hong,¹⁷ M. A. Mazur,¹⁷ J. D. Richman,¹⁷ W. Verkerke,¹⁷
T. W. Beck,¹⁸ A. M. Eisner,¹⁸ C. J. Flacco,¹⁸ C. A. Heusch,¹⁸ J. Kroseberg,¹⁸ W. S. Lockman,¹⁸ G. Nesom,¹⁸
T. Schalk,¹⁸ B. A. Schumm,¹⁸ A. Seiden,¹⁸ P. Spradlin,¹⁸ D. C. Williams,¹⁸ M. G. Wilson,¹⁸ J. Albert,¹⁹
E. Chen,¹⁹ G. P. Dubois-Felsmann,¹⁹ A. Dvoretskii,¹⁹ D. G. Hitlin,¹⁹ I. Narsky,¹⁹ T. Piatenko,¹⁹ F. C. Porter,¹⁹
A. Ryd,¹⁹ A. Samuel,¹⁹ R. Andreassen,²⁰ S. Jayatilleke,²⁰ G. Mancinelli,²⁰ B. T. Meadows,²⁰ M. D. Sokoloff,²⁰
F. Blanc,²¹ P. Bloom,²¹ S. Chen,²¹ W. T. Ford,²¹ U. Nauenberg,²¹ A. Olivas,²¹ P. Rankin,²¹ W. O. Ruddick,²¹
J. G. Smith,²¹ K. A. Ulmer,²¹ S. R. Wagner,²¹ J. Zhang,²¹ A. Chen,²² E. A. Eckhart,²² A. Soffer,²² W. H. Toki,²²
R. J. Wilson,²² Q. Zeng,²² D. Altenburg,²³ E. Feltresi,²³ A. Hauke,²³ B. Spaan,²³ T. Brandt,²⁴ J. Brose,²⁴
M. Dickopp,²⁴ V. Klose,²⁴ H. M. Lacker,²⁴ R. Nogowski,²⁴ S. Otto,²⁴ A. Petzold,²⁴ G. Schott,²⁴ J. Schubert,²⁴
K. R. Schubert,²⁴ R. Schwierz,²⁴ J. E. Sundermann,²⁴ D. Bernard,²⁵ G. R. Bonneau,²⁵ P. Grenier,²⁵ S. Schrenk,²⁵
Ch. Thiebaux,²⁵ G. Vasileiadis,²⁵ M. Verderi,²⁵ D. J. Bard,²⁶ P. J. Clark,²⁶ W. Gradl,²⁶ F. Muheim,²⁶ S. Playfer,²⁶
Y. Xie,²⁶ M. Andreotti,²⁷ V. Azzolini,²⁷ D. Bettoni,²⁷ C. Bozzi,²⁷ R. Calabrese,²⁷ G. Cibinetto,²⁷ E. Luppi,²⁷
M. Negrini,²⁷ L. Piemontese,²⁷ F. Anulli,²⁸ R. Baldini-Ferroli,²⁸ A. Calcaterra,²⁸ R. de Sangro,²⁸ G. Finocchiaro,²⁸
P. Patteri,²⁸ I. M. Peruzzi,²⁸, * M. Piccolo,²⁸ A. Zallo,²⁸ A. Buzzo,²⁹ R. Capra,²⁹ R. Contri,²⁹ M. Lo Vetere,²⁹
M. Macri,²⁹ M. R. Monge,²⁹ S. Passaggio,²⁹ C. Patrignani,²⁹ E. Robutti,²⁹ A. Santroni,²⁹ S. Tosi,²⁹ S. Bailey,³⁰
G. Brandenburg,³⁰ K. S. Chaisanguanthum,³⁰ M. Morii,³⁰ E. Won,³⁰ J. Wu,³⁰ R. S. Dubitzky,³¹ U. Langenegger,³¹
J. Marks,³¹ S. Schenk,³¹ U. Uwer,³¹ W. Bhimji,³² D. A. Bowerman,³² P. D. Dauncey,³² U. Egede,³² R. L. Flack,³²
J. R. Gaillard,³² G. W. Morton,³² J. A. Nash,³² M. B. Nikolich,³² G. P. Taylor,³² W. P. Vazquez,³² M. J. Charles,³³
W. F. Mader,³³ U. Mallik,³³ A. K. Mohapatra,³³ J. Cochran,³⁴ H. B. Crawley,³⁴ V. Eges,³⁴ W. T. Meyer,³⁴
S. Prell,³⁴ E. I. Rosenberg,³⁴ A. E. Rubin,³⁴ J. Yi,³⁴ N. Arnaud,³⁵ M. Davier,³⁵ X. Giroux,³⁵ G. Grosdidier,³⁵
A. Höcker,³⁵ F. Le Diberder,³⁵ V. Lepeltier,³⁵ A. M. Lutz,³⁵ A. Oyanguren,³⁵ T. C. Petersen,³⁵ M. Pierini,³⁵
S. Plaszczynski,³⁵ S. Rodier,³⁵ P. Roudeau,³⁵ M. H. Schune,³⁵ A. Stocchi,³⁵ G. Wormser,³⁵ C. H. Cheng,³⁶
D. J. Lange,³⁶ M. C. Simani,³⁶ D. M. Wright,³⁶ A. J. Bevan,³⁷ C. A. Chavez,³⁷ J. P. Coleman,³⁷ I. J. Forster,³⁷
J. R. Fry,³⁷ E. Gabathuler,³⁷ R. Gamet,³⁷ K. A. George,³⁷ D. E. Hutchcroft,³⁷ R. J. Parry,³⁷ D. J. Payne,³⁷
K. C. Schofield,³⁷ C. Touramanis,³⁷ C. M. Cormack,³⁸ F. Di Lodovico,³⁸ R. Sacco,³⁸ C. L. Brown,³⁹ G. Cowan,³⁹
H. U. Flaecher,³⁹ M. G. Green,³⁹ D. A. Hopkins,³⁹ P. S. Jackson,³⁹ T. R. McMahon,³⁹ S. Ricciardi,³⁹ F. Salvatore,³⁹
D. Brown,⁴⁰ C. L. Davis,⁴⁰ J. Allison,⁴¹ N. R. Barlow,⁴¹ R. J. Barlow,⁴¹ M. C. Hodgkinson,⁴¹ G. D. Lafferty,⁴¹
M. T. Naisbit,⁴¹ J. C. Williams,⁴¹ C. Chen,⁴² A. Farbin,⁴² W. D. Hulsbergen,⁴² A. Jawahery,⁴² D. Kovalskyi,⁴²
C. K. Lae,⁴² V. Lillard,⁴² D. A. Roberts,⁴² G. Simi,⁴² G. Blaylock,⁴³ C. Dallapiccola,⁴³ S. S. Hertzbach,⁴³

R. Kofler,⁴³ V. B. Koptchev,⁴³ X. Li,⁴³ T. B. Moore,⁴³ S. Saremi,⁴³ H. Staengle,⁴³ S. Willocq,⁴³ R. Cowan,⁴⁴
 K. Koenenke,⁴⁴ G. Sciolla,⁴⁴ S. J. Sekula,⁴⁴ M. Spitznagel,⁴⁴ F. Taylor,⁴⁴ R. K. Yamamoto,⁴⁴ H. Kim,⁴⁵ P. M. Patel,⁴⁵
 S. H. Robertson,⁴⁵ A. Lazzaro,⁴⁶ V. Lombardo,⁴⁶ F. Palombo,⁴⁶ J. M. Bauer,⁴⁷ L. Cremaldi,⁴⁷ V. Eschenburg,⁴⁷
 R. Godang,⁴⁷ R. Kroeger,⁴⁷ J. Reidy,⁴⁷ D. A. Sanders,⁴⁷ D. J. Summers,⁴⁷ H. W. Zhao,⁴⁷ S. Brunet,⁴⁸ D. Côté,⁴⁸
 P. Taras,⁴⁸ B. Viaud,⁴⁸ H. Nicholson,⁴⁹ N. Cavallo,⁵⁰, † G. De Nardo,⁵⁰ F. Fabozzi,⁵⁰, † C. Gatto,⁵⁰ L. Lista,⁵⁰
 D. Monorchio,⁵⁰ P. Paolucci,⁵⁰ D. Piccolo,⁵⁰ C. Sciacca,⁵⁰ M. Baak,⁵¹ H. Bulten,⁵¹ G. Raven,⁵¹ H. L. Snoek,⁵¹
 L. Wilden,⁵¹ C. P. Jessop,⁵² J. M. LoSecco,⁵² T. Allmendinger,⁵³ G. Benelli,⁵³ K. K. Gan,⁵³ K. Honscheid,⁵³
 D. Hufnagel,⁵³ P. D. Jackson,⁵³ H. Kagan,⁵³ R. Kass,⁵³ T. Pulliam,⁵³ A. M. Rahimi,⁵³ R. Ter-Antonyan,⁵³
 Q. K. Wong,⁵³ J. Brau,⁵⁴ R. Frey,⁵⁴ O. Igonkina,⁵⁴ M. Lu,⁵⁴ C. T. Potter,⁵⁴ N. B. Sinev,⁵⁴ D. Strom,⁵⁴ J. Strube,⁵⁴
 E. Torrence,⁵⁴ A. Dorigo,⁵⁵ F. Galeazzi,⁵⁵ M. Margoni,⁵⁵ M. Morandin,⁵⁵ M. Posocco,⁵⁵ M. Rotondo,⁵⁵
 F. Simonetto,⁵⁵ R. Stroili,⁵⁵ C. Voci,⁵⁵ M. Benayoun,⁵⁶ H. Briand,⁵⁶ J. Chauveau,⁵⁶ P. David,⁵⁶ L. Del Buono,⁵⁶
 Ch. de la Vaissière,⁵⁶ O. Hamon,⁵⁶ M. J. J. John,⁵⁶ Ph. Leruste,⁵⁶ J. Malclès,⁵⁶ J. Ocariz,⁵⁶ L. Roos,⁵⁶ G. Therin,⁵⁶
 P. K. Behera,⁵⁷ L. Gladney,⁵⁷ Q. H. Guo,⁵⁷ J. Panetta,⁵⁷ M. Biasini,⁵⁸ R. Covarelli,⁵⁸ S. Pacetti,⁵⁸ M. Pioppi,⁵⁸
 C. Angelini,⁵⁹ G. Batignani,⁵⁹ S. Bettarini,⁵⁹ F. Bucci,⁵⁹ G. Calderini,⁵⁹ M. Carpinelli,⁵⁹ R. Cenci,⁵⁹ F. Forti,⁵⁹
 M. A. Giorgi,⁵⁹ A. Lusiani,⁵⁹ G. Marchiori,⁵⁹ M. Morganti,⁵⁹ N. Neri,⁵⁹ E. Paoloni,⁵⁹ M. Rama,⁵⁹ G. Rizzo,⁵⁹
 J. Walsh,⁵⁹ M. Haire,⁶⁰ D. Judd,⁶⁰ D. E. Wagoner,⁶⁰ J. Biesiada,⁶¹ N. Danielson,⁶¹ P. Elmer,⁶¹ Y. P. Lau,⁶¹
 C. Lu,⁶¹ J. Olsen,⁶¹ A. J. S. Smith,⁶¹ A. V. Telnov,⁶¹ F. Bellini,⁶² G. Cavoto,⁶² A. D’Orazio,⁶² E. Di Marco,⁶²
 R. Faccini,⁶² F. Ferrarotto,⁶² F. Ferroni,⁶² M. Gaspero,⁶² L. Li Gioi,⁶² M. A. Mazzoni,⁶² S. Morganti,⁶²
 G. Piredda,⁶² F. Polci,⁶² F. Safai Tehrani,⁶² C. Vena,⁶² H. Schröder,⁶³ G. Wagner,⁶³ R. Waldi,⁶³ T. Adye,⁶⁴ N. De
 Groot,⁶⁴ B. Franek,⁶⁴ G. P. Gopal,⁶⁴ E. O. Olaiya,⁶⁴ F. F. Wilson,⁶⁴ R. Aleksan,⁶⁵ S. Emery,⁶⁵ A. Gaidot,⁶⁵
 S. F. Ganzhur,⁶⁵ P.-F. Giraud,⁶⁵ G. Graziani,⁶⁵ G. Hamel de Monchenault,⁶⁵ W. Kozanecki,⁶⁵ M. Legendre,⁶⁵
 G. W. London,⁶⁵ B. Mayer,⁶⁵ G. Vasseur,⁶⁵ Ch. Yèche,⁶⁵ M. Zito,⁶⁵ M. V. Purohit,⁶⁶ A. W. Weidemann,⁶⁶
 J. R. Wilson,⁶⁶ F. X. Yumiceva,⁶⁶ T. Abe,⁶⁷ M. T. Allen,⁶⁷ D. Aston,⁶⁷ R. Bartoldus,⁶⁷ N. Berger,⁶⁷
 A. M. Boyarski,⁶⁷ O. L. Buchmueller,⁶⁷ R. Claus,⁶⁷ M. R. Convery,⁶⁷ M. Cristinziani,⁶⁷ J. C. Dingfelder,⁶⁷
 D. Dong,⁶⁷ J. Dorfan,⁶⁷ D. Dujmic,⁶⁷ W. Dunwoodie,⁶⁷ S. Fan,⁶⁷ R. C. Field,⁶⁷ T. Glanzman,⁶⁷ S. J. Gowdy,⁶⁷
 T. Hadig,⁶⁷ V. Halyo,⁶⁷ C. Hast,⁶⁷ T. Hrynn’ova,⁶⁷ W. R. Innes,⁶⁷ M. H. Kelsey,⁶⁷ P. Kim,⁶⁷ M. L. Kocian,⁶⁷
 D. W. G. S. Leith,⁶⁷ J. Libby,⁶⁷ S. Luitz,⁶⁷ V. Luth,⁶⁷ H. L. Lynch,⁶⁷ H. Marsiske,⁶⁷ R. Messner,⁶⁷ D. R. Muller,⁶⁷
 C. P. O’Grady,⁶⁷ V. E. Ozcan,⁶⁷ A. Perazzo,⁶⁷ M. Perl,⁶⁷ B. N. Ratcliff,⁶⁷ A. Roodman,⁶⁷ A. A. Salnikov,⁶⁷
 R. H. Schindler,⁶⁷ J. Schwiening,⁶⁷ A. Snyder,⁶⁷ J. Stelzer,⁶⁷ D. Su,⁶⁷ M. K. Sullivan,⁶⁷ K. Suzuki,⁶⁷ S. Swain,⁶⁷
 J. M. Thompson,⁶⁷ J. Va’vra,⁶⁷ M. Weaver,⁶⁷ W. J. Wisniewski,⁶⁷ M. Wittgen,⁶⁷ D. H. Wright,⁶⁷ A. K. Yarritu,⁶⁷
 K. Yi,⁶⁷ C. C. Young,⁶⁷ P. R. Burchat,⁶⁸ A. J. Edwards,⁶⁸ S. A. Majewski,⁶⁸ B. A. Petersen,⁶⁸ C. Roat,⁶⁸
 M. Ahmed,⁶⁹ S. Ahmed,⁶⁹ M. S. Alam,⁶⁹ J. A. Ernst,⁶⁹ M. A. Saeed,⁶⁹ F. R. Wappler,⁶⁹ S. B. Zain,⁶⁹ W. Bugg,⁷⁰
 M. Krishnamurthy,⁷⁰ S. M. Spanier,⁷⁰ R. Eckmann,⁷¹ J. L. Ritchie,⁷¹ A. Satpathy,⁷¹ R. F. Schwitters,⁷¹
 J. M. Izen,⁷² I. Kitayama,⁷² X. C. Lou,⁷² S. Ye,⁷² F. Bianchi,⁷³ M. Bona,⁷³ F. Gallo,⁷³ D. Gamba,⁷³ M. Bomben,⁷⁴
 L. Bosisio,⁷⁴ C. Cartaro,⁷⁴ F. Cossutti,⁷⁴ G. Della Ricca,⁷⁴ S. Dittongo,⁷⁴ S. Grancagnolo,⁷⁴ L. Lanceri,⁷⁴
 L. Vitale,⁷⁴ F. Martinez-Vidal,⁷⁵ R. S. Panvini,⁷⁶, † Sw. Banerjee,⁷⁷ B. Bhuyan,⁷⁷ C. M. Brown,⁷⁷ D. Fortin,⁷⁷
 K. Hamano,⁷⁷ R. Kowalewski,⁷⁷ J. M. Roney,⁷⁷ R. J. Sobie,⁷⁷ J. J. Back,⁷⁸ P. F. Harrison,⁷⁸ T. E. Latham,⁷⁸
 G. B. Mohanty,⁷⁸ H. R. Band,⁷⁹ X. Chen,⁷⁹ B. Cheng,⁷⁹ S. Dasu,⁷⁹ M. Datta,⁷⁹ A. M. Eichenbaum,⁷⁹ K. T. Flood,⁷⁹
 M. Graham,⁷⁹ J. J. Hollar,⁷⁹ J. R. Johnson,⁷⁹ P. E. Kutter,⁷⁹ H. Li,⁷⁹ R. Liu,⁷⁹ B. Mellado,⁷⁹ A. Mihalyi,⁷⁹
 Y. Pan,⁷⁹ R. Prepost,⁷⁹ P. Tan,⁷⁹ J. H. von Wimmersperg-Toeller,⁷⁹ S. L. Wu,⁷⁹ Z. Yu,⁷⁹ and H. Neal⁸⁰

(The BABAR Collaboration)

¹Laboratoire de Physique des Particules, F-74941 Annecy-le-Vieux, France

²IFAE, Universitat Autònoma de Barcelona, E-08193 Bellaterra, Barcelona, Spain

³Università di Bari, Dipartimento di Fisica and INFN, I-70126 Bari, Italy

⁴Institute of High Energy Physics, Beijing 100039, China

⁵University of Bergen, Inst. of Physics, N-5007 Bergen, Norway

⁶Lawrence Berkeley National Laboratory and University of California, Berkeley, California 94720, USA

⁷University of Birmingham, Birmingham, B15 2TT, United Kingdom

⁸Ruhr Universität Bochum, Institut für Experimentalphysik 1, D-44780 Bochum, Germany

⁹University of Bristol, Bristol BS8 1TL, United Kingdom

¹⁰University of British Columbia, Vancouver, British Columbia, Canada V6T 1Z1

¹¹Brunel University, Uxbridge, Middlesex UB8 3PH, United Kingdom

¹²Budker Institute of Nuclear Physics, Novosibirsk 630090, Russia

¹³University of California at Irvine, Irvine, California 92697, USA

- ¹⁴University of California at Los Angeles, Los Angeles, California 90024, USA
¹⁵University of California at Riverside, Riverside, California 92521, USA
¹⁶University of California at San Diego, La Jolla, California 92093, USA
¹⁷University of California at Santa Barbara, Santa Barbara, California 93106, USA
¹⁸University of California at Santa Cruz, Institute for Particle Physics, Santa Cruz, California 95064, USA
¹⁹California Institute of Technology, Pasadena, California 91125, USA
²⁰University of Cincinnati, Cincinnati, Ohio 45221, USA
²¹University of Colorado, Boulder, Colorado 80309, USA
²²Colorado State University, Fort Collins, Colorado 80523, USA
²³Universität Dortmund, Institut für Physik, D-44221 Dortmund, Germany
²⁴Technische Universität Dresden, Institut für Kern- und Teilchenphysik, D-01062 Dresden, Germany
²⁵Ecole Polytechnique, LLR, F-91128 Palaiseau, France
²⁶University of Edinburgh, Edinburgh EH9 3JZ, United Kingdom
²⁷Università di Ferrara, Dipartimento di Fisica and INFN, I-44100 Ferrara, Italy
²⁸Laboratori Nazionali di Frascati dell'INFN, I-00044 Frascati, Italy
²⁹Università di Genova, Dipartimento di Fisica and INFN, I-16146 Genova, Italy
³⁰Harvard University, Cambridge, Massachusetts 02138, USA
³¹Universität Heidelberg, Physikalisches Institut, Philosophenweg 12, D-69120 Heidelberg, Germany
³²Imperial College London, London, SW7 2AZ, United Kingdom
³³University of Iowa, Iowa City, Iowa 52242, USA
³⁴Iowa State University, Ames, Iowa 50011-3160, USA
³⁵Laboratoire de l'Accélérateur Linéaire, F-91898 Orsay, France
³⁶Lawrence Livermore National Laboratory, Livermore, California 94550, USA
³⁷University of Liverpool, Liverpool L69 7ZE, United Kingdom
³⁸Queen Mary, University of London, E1 4NS, United Kingdom
³⁹University of London, Royal Holloway and Bedford New College, Egham, Surrey TW20 0EX, United Kingdom
⁴⁰University of Louisville, Louisville, Kentucky 40292, USA
⁴¹University of Manchester, Manchester M13 9PL, United Kingdom
⁴²University of Maryland, College Park, Maryland 20742, USA
⁴³University of Massachusetts, Amherst, Massachusetts 01003, USA
⁴⁴Massachusetts Institute of Technology, Laboratory for Nuclear Science, Cambridge, Massachusetts 02139, USA
⁴⁵McGill University, Montréal, Quebec, Canada H3A 2T8
⁴⁶Università di Milano, Dipartimento di Fisica and INFN, I-20133 Milano, Italy
⁴⁷University of Mississippi, University, Mississippi 38677, USA
⁴⁸Université de Montréal, Laboratoire René J. A. Lévesque, Montréal, Quebec, Canada H3C 3J7
⁴⁹Mount Holyoke College, South Hadley, Massachusetts 01075, USA
⁵⁰Università di Napoli Federico II, Dipartimento di Scienze Fisiche and INFN, I-80126, Napoli, Italy
⁵¹NIKHEF, National Institute for Nuclear Physics and High Energy Physics, NL-1009 DB Amsterdam, The Netherlands
⁵²University of Notre Dame, Notre Dame, Indiana 46556, USA
⁵³Ohio State University, Columbus, Ohio 43210, USA
⁵⁴University of Oregon, Eugene, Oregon 97403, USA
⁵⁵Università di Padova, Dipartimento di Fisica and INFN, I-35131 Padova, Italy
⁵⁶Universités Paris VI et VII, Laboratoire de Physique Nucléaire et de Hautes Energies, F-75252 Paris, France
⁵⁷University of Pennsylvania, Philadelphia, Pennsylvania 19104, USA
⁵⁸Università di Perugia, Dipartimento di Fisica and INFN, I-06100 Perugia, Italy
⁵⁹Università di Pisa, Dipartimento di Fisica, Scuola Normale Superiore and INFN, I-56127 Pisa, Italy
⁶⁰Prairie View A&M University, Prairie View, Texas 77446, USA
⁶¹Princeton University, Princeton, New Jersey 08544, USA
⁶²Università di Roma La Sapienza, Dipartimento di Fisica and INFN, I-00185 Roma, Italy
⁶³Universität Rostock, D-18051 Rostock, Germany
⁶⁴Rutherford Appleton Laboratory, Chilton, Didcot, Oxon, OX11 0QX, United Kingdom
⁶⁵DSM/Dapnia, CEA/Saclay, F-91191 Gif-sur-Yvette, France
⁶⁶University of South Carolina, Columbia, South Carolina 29208, USA
⁶⁷Stanford Linear Accelerator Center, Stanford, California 94309, USA
⁶⁸Stanford University, Stanford, California 94305-4060, USA
⁶⁹State University of New York, Albany, New York 12222, USA
⁷⁰University of Tennessee, Knoxville, Tennessee 37996, USA
⁷¹University of Texas at Austin, Austin, Texas 78712, USA
⁷²University of Texas at Dallas, Richardson, Texas 75083, USA
⁷³Università di Torino, Dipartimento di Fisica Sperimentale and INFN, I-10125 Torino, Italy
⁷⁴Università di Trieste, Dipartimento di Fisica and INFN, I-34127 Trieste, Italy
⁷⁵IFIC, Universitat de Valencia-CSIC, E-46071 Valencia, Spain
⁷⁶Vanderbilt University, Nashville, Tennessee 37235, USA
⁷⁷University of Victoria, Victoria, British Columbia, Canada V8W 3P6

⁷⁸Department of Physics, University of Warwick, Coventry CV4 7AL, United Kingdom

⁷⁹University of Wisconsin, Madison, Wisconsin 53706, USA

⁸⁰Yale University, New Haven, Connecticut 06511, USA

(Dated: February 4, 2020)

With a sample of 232×10^6 $\Upsilon(4S) \rightarrow B\bar{B}$ events collected with the *BABAR* detector, we study the decay $B^+ \rightarrow p\bar{p}K^+$ excluding charmonium decays to $p\bar{p}$. We measure a branching fraction $\mathcal{B}(B^+ \rightarrow p\bar{p}K^+) = (6.7 \pm 0.5 \pm 0.4) \times 10^{-6}$. An enhancement at low $p\bar{p}$ mass is observed and the Dalitz plot asymmetry suggests dominance of the penguin amplitude in this B decay. We search for a pentaquark candidate Θ^{*++} decaying into pK^+ in the mass range 1.43 to 2.00 GeV/c^2 and set limits on $\mathcal{B}(B^+ \rightarrow \Theta^{*++}\bar{p}) \times \mathcal{B}(\Theta^{*++} \rightarrow pK^+)$ at the 10^{-7} level.

PACS numbers: 13.25.Hw, 12.15.Hh, 11.30.Er

This paper describes a measurement of the branching fraction of the baryonic three-body decay $B^+ \rightarrow p\bar{p}K^+$ [1] (excluding charmonium decays to $p\bar{p}$) and a study of its resonant substructure. An earlier measurement [2] of the branching fraction for this channel gave $(5.7^{+0.7}_{-0.6} \pm 0.7) \times 10^{-6}$. This channel is interesting for the dynamical information in the distribution of the three final-state particles and for the possible presence of exotic [3], [4] intermediate states. We also isolate decays $B^+ \rightarrow X_{c\bar{c}}K^+$, where $X_{c\bar{c}} = \eta_c$ and J/ψ decaying to $p\bar{p}$, and measure the width of the η_c .

An important feature of this decay is an enhancement at low $p\bar{p}$ masses reported in Ref. [2], similar to those that have been observed in several other baryonic decays of B [5] and J/ψ [6]. This could be a feature of a quasi-two-body decay in which the $p\bar{p}$ system is produced through an intermediate gluonic resonance [3] (Fig. 1(c)). It could also be that the decay is a pure three-body process and that the enhancement results from the short-range correlations between p and \bar{p} in the fragmentation chain [7], [8]. Rosner suggested [9] that it is possible to distinguish the fragmentation or gluonic resonance mechanisms by studying the distribution of events in the Dalitz plot.

The main Feynman diagrams for this decay are presented in Fig. 1. The leading diagrams [8] are a penguin diagram and a doubly Cabibbo-Kobayashi-Maskawa-suppressed tree diagram shown in Fig. 1(a,b). There is also an Okubo-Zweig-Iizuka-suppressed penguin diagram shown in Fig. 1(c), where the $p\bar{p}$ pair is created through a pair of gluons (or a gluonic resonance). There are four additional color-suppressed diagrams [8]: two tree diagrams with an internal W^+ -emission and a W^+ -annihilation and two penguin diagrams with an internal gluon-emission that are expected to be small. If the $p\bar{p}$ system is produced independently of the K^+ through a tree diagram with an external W^+ -emission (Fig. 1(b)) or a penguin with an external gluon-emission (Fig. 1(c)), i.e. the $p\bar{p}$ quark lines are not associated with the \bar{s} or u quarks in the K^+ , then the distributions m_{pK^+} and $m_{\bar{p}K^+}$ should be identical. If the u quark in the K^+ is associated with a \bar{u} quark in a \bar{p} (Fig. 1(a)), larger values of m_{pK^+} are favored over those of $m_{\bar{p}K^+}$ [9]. Thus a study of the Dalitz plot provides insight not only into the

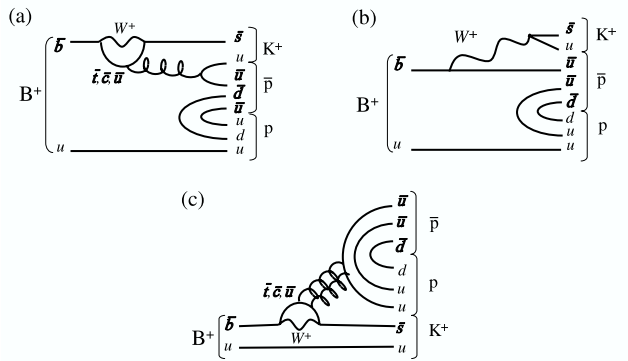


FIG. 1: The main Feynman diagrams for the non-resonant $B^+ \rightarrow p\bar{p}K^+$ decay: (a) leading penguin diagram, (b) leading tree diagram (external W^+ -emission), (c) Okubo-Zweig-Iizuka-suppressed penguin diagram.

dominant mechanism of this decay but also into whether the penguin or the tree amplitude is dominant.

This paper is organized as follows: first we describe the event selection and the branching-fraction measurement. Then we describe the $p\bar{p}$ mass spectrum and the measurement of the η_c width. We examine the Dalitz plot for an asymmetry between the distributions in m_{pK^+} and $m_{\bar{p}K^+}$. In the final section we describe searches for $B^+ \rightarrow p\bar{\Lambda}(1520) \rightarrow p(\bar{p}K^+)$ decay and for the hypothesized $I = 1$, $I_3 = 1$ pentaquark state Θ^{*++} (a member of the baryon 27-plet with quark content $uuuds\bar{s}$) in the decay $B^+ \rightarrow \Theta^{*++}\bar{p} \rightarrow (pK^+)\bar{p}$. The Θ^{*++} mass has been predicted [10] to lie in the region $1.43 - 1.70 \text{ GeV}/c^2$.

The analysis uses 232×10^6 $\Upsilon(4S) \rightarrow B\bar{B}$ decays collected with the *BABAR* detector [11] at the PEP-II e^+e^- storage ring. Charged tracks are measured by a five-layer silicon vertex tracker (SVT) and a 40-layer drift-chamber (DCH) in a 1.5-T solenoidal magnetic field. A Cherenkov radiation detector (DIRC) is used for charged-particle identification. The CsI(Tl) electromagnetic calorimeter detects photon and electron showers. To identify kaons and protons we use dE/dx measurements in the SVT and DCH, and the pattern of Cherenkov photons in the DIRC. The proton efficiency is 93% with 9% kaon misidentification probability. The kaon efficiency is 87% with 2% pion misidentification probability.

We use the kinematic constraints of B -meson pair-production at the $\Upsilon(4S)$ to identify the $B^+ \rightarrow p\bar{p}K^+$ signal. Two independent variables are calculated for each $p\bar{p}K^+$ candidate: $m_{ES} = [(E_{cm}^2/2 + \mathbf{p}_0 \cdot \mathbf{p}_B)^2/E_0^2 - \mathbf{p}_B^2]^{1/2}$ and $\Delta E = E_B^* - E_{cm}/2$, where E_{cm} is the total center-of-mass energy, the subscripts 0 and B refer to the initial $\Upsilon(4S)$ and to the B candidate, respectively, and the asterisk denotes the $\Upsilon(4S)$ frame. The resolutions on ΔE and m_{ES} are about 17 MeV and 2.6 MeV/ c^2 , respectively.

Backgrounds arise primarily from random combinations in continuum events ($e^+e^- \rightarrow q\bar{q}$, where $q = u, d, s, c$). These events are collimated along the original quark directions and can be distinguished from more spherical $B\bar{B}$ events with a Fisher discriminant (\mathcal{F}) [12], a linear combination of four event-shape variables. The four variables are $\cos\theta_{thr}^*$, the angle between the thrust axis of the reconstructed B and the beam axis; $\cos\theta_{mom}^*$, the angle between the momentum of the reconstructed B and the beam axis; and the zeroth and second Legendre polynomial momentum moments, $L_0 = \sum_i |\mathbf{p}_i^*|$ and $L_2 = \sum_i |\mathbf{p}_i^*|[(3\cos^2\theta_{thrB,i}^* - 1)/2]$, where \mathbf{p}_i^* are the momenta of the tracks and neutral clusters not associated with the B candidate and $\theta_{thrB,i}^*$ is the angle between \mathbf{p}_i^* and the thrust axis of the B candidate. The event selection is optimized assuming the previously measured value of the branching fraction [2] to maximize $s/\sqrt{s+b}$, where s and b are the expected number of signal and background events, respectively. The event selection retains 66% of signal events while removing 93% of continuum background.

The resulting distribution of events in the m_{ES} – ΔE plane is shown in Fig. 2. A clear signal is observed at the B mass and $\Delta E=0$. Potential backgrounds are studied with Monte Carlo (MC) simulation [14]. The combinatorial background is expected to come predominantly (89%) from continuum events. Background events in the signal region arise mostly from $B^+ \rightarrow X_{c\bar{c}}(p\bar{p})K^+$, where $X_{c\bar{c}} = \eta_c, J/\psi, \psi', \chi_{c0,1,2}$ (the charmonium background), while non-charmonium B backgrounds are expected to be negligible. The signal and sideband regions are defined to be “wide” ($5.27 < m_{ES} < 5.29 \text{ GeV}/c^2$ and $5.20 < m_{ES} < 5.26 \text{ GeV}/c^2$, $|\Delta E| < 50 \text{ MeV}$) for the charmonium background studies and “narrow” ($5.276 < m_{ES} < 5.286 \text{ GeV}/c^2$ and $5.20 < m_{ES} < 5.26 \text{ GeV}/c^2$, $|\Delta E| < 29 \text{ MeV}$) for the Dalitz plot study.

To extract the $p\bar{p}K^+$ signal yield, we fit the ΔE distributions for candidates that lie in the $5.27 < m_{ES} < 5.29 \text{ GeV}/c^2$ region separately in nine bins of $m_{p\bar{p}}$. The size of the bins is shown in Fig. 3. We use a linear function for the background and a double Gaussian distribution for the signal. The widths and means of the Gaussian distributions and their relative areas are fixed to values obtained from MC simulation, which is also used to calculate the detection efficiency ($\varepsilon_{m_{p\bar{p}}}$) in each $m_{p\bar{p}}$ bin. Across the allowed kinematic region, $\varepsilon_{m_{p\bar{p}}}$

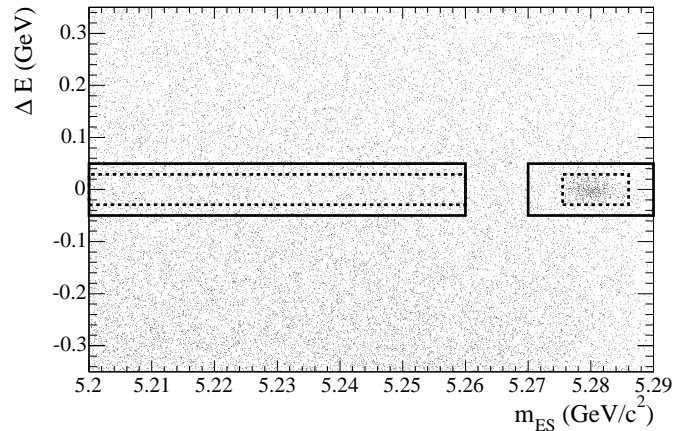


FIG. 2: Distribution of ΔE versus m_{ES} for the $p\bar{p}K^+$ candidates in data. The solid (dashed) lines define the wide (narrow) signal and sideband regions.

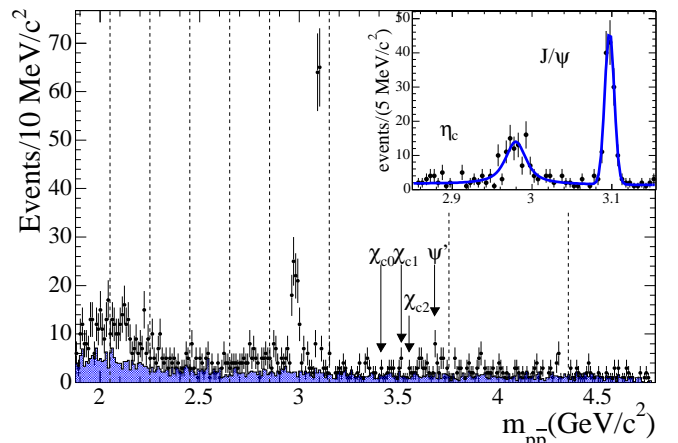


FIG. 3: The $m_{p\bar{p}}$ distribution for data in the wide signal (points) and sideband (shade) regions. The sideband histogram is scaled to the expected number of the combinatorial background events in the signal region.

declines smoothly from 30% at threshold to 24% at the highest mass. The ΔE fits for $m_{p\bar{p}}$ below $2.85 \text{ GeV}/c^2$ yield 343^{+27}_{-26} signal events. From the known number of charged B mesons in the sample, the branching fraction for $m_{p\bar{p}}$ below the η_c mass is measured to be $\mathcal{B}(B^+ \rightarrow p\bar{p}K^+; m_{p\bar{p}} < 2.85 \text{ GeV}/c^2) = (5.3 \pm 0.4 \pm 0.3) \times 10^{-6}$.

An estimate of the number of charmonium events in the $m_{p\bar{p}} > 2.85 \text{ GeV}/c^2$ region is required to determine the total non-charmonium branching fraction. To minimize the systematic error on that quantity, we fit the $m_{p\bar{p}}$ spectrum for the number of the non-charmonium events in the primary “charmonium” region ($2.85 < m_{p\bar{p}} < 3.15 \text{ GeV}/c^2$). To improve the $p\bar{p}$ mass resolution in the $m_{p\bar{p}}$ fit, we perform a kinematic fit fixing the mass and energy of each B candidate in the wide signal and sideband regions to their known values. The $m_{p\bar{p}}$ distribution is shown in Fig. 3, where prominent signals for the η_c and J/ψ decaying into $p\bar{p}$ are visible. The region used in the $m_{p\bar{p}}$ fit, $2.4 < m_{p\bar{p}} < 3.4 \text{ GeV}/c^2$, is chosen wider than the “charmonium” region of inter-

est ($2.85 < m_{p\bar{p}} < 3.15 \text{ GeV}/c^2$), shown in Fig. 3(inset), to improve the statistical uncertainties on the $p\bar{p}K^+$ signal and combinatorial background yield. The η_c peak is described by a convolution of a Breit-Wigner distribution and a Gaussian distribution, and the J/ψ peak by a sum of two Gaussian distributions with a common mean. The shapes are obtained from MC simulation. The width of the broader J/ψ Gaussian distribution and ratio of areas of the two J/ψ Gaussian distributions are constrained in the fit to their MC values. A common width is used for the narrow Gaussian distributions for J/ψ and η_c and is a free parameter in the fit. The $p\bar{p}K^+$ signal and combinatorial background distributions are modeled by a linear function of $m_{p\bar{p}}$. The inset of Fig. 3 shows this fit, which results in 114^{+15}_{-14} η_c events and 137^{+13}_{-12} J/ψ events. Correcting for the detection efficiency of $(26.9 \pm 0.2)\%$, we find $\mathcal{B}(B^+ \rightarrow \eta_c K^+) \times \mathcal{B}(\eta_c \rightarrow p\bar{p}) = (1.8^{+0.3}_{-0.2} \pm 0.2) \times 10^{-6}$ and $\mathcal{B}(B^+ \rightarrow J/\psi K^+) \times \mathcal{B}(J/\psi \rightarrow p\bar{p}) = (2.2 \pm 0.2 \pm 0.1) \times 10^{-6}$ in agreement with the accepted values [13]. The fit yields a total η_c width of $\Gamma(\eta_c) = 25^{+6}_{-5} \pm 3 \text{ MeV}/c^2$ consistent with the current values [13] and a mass resolution of $5.7 \pm 0.4 \text{ MeV}/c^2$ in agreement with MC expectations.

The $m_{p\bar{p}}$ fit yields 88 ± 6 $p\bar{p}K^+$ signal and combinatorial background events in the charmonium region (see Fig. 3). In this region, the latter contribution is estimated from the ΔE fit to be 53 ± 5 events, resulting in a non-charmonium $p\bar{p}K^+$ signal of 35 ± 8 events. The contribution from higher-mass charmonium modes is estimated to be 24 ± 5 events from the accepted [13] values for their branching fractions. Adding the $p\bar{p}K^+$ signal yield obtained from the ΔE fits outside the “charmonium” region with non-charmonium $p\bar{p}K^+$ signal in the “charmonium” region, and subtracting the contribution of the higher mass charmonium modes results in a total non-charmonium signal yield of 433 ± 33 events. Correcting the signal yield for efficiency in each of the $m_{p\bar{p}}$ bins and normalizing to the number of B^+ mesons in the data sample results in a total branching fraction of $\mathcal{B}(B^+ \rightarrow p\bar{p}K^+) = (6.7 \pm 0.5 \pm 0.4) \times 10^{-6}$ with charmonium decays to $p\bar{p}$ excluded. Figure 4 shows the background-subtracted and efficiency-corrected $p\bar{p}$ mass spectrum and the expectation for a three-body phase-space decay. The existence of a low-mass enhancement in the $p\bar{p}$ mass as previously observed by Belle [2] is confirmed.

The charge asymmetry is defined as $A_{ch} = (N_{B^-} - N_{B^+}) / (N_{B^-} + N_{B^+})$, where N_{B^\pm} is the number of $B^\pm \rightarrow p\bar{p}K^\pm$ events. We use the same fitting procedure as for the branching fraction measurement, and find $A_{ch} = -0.16^{+0.07}_{-0.08} \pm 0.04$ for $m_{p\bar{p}} < 2.85 \text{ GeV}/c^2$.

For the remainder of this paper to increase the signal purity, only events in the narrow signal and m_{ES} -sideband regions are considered. After selecting the B candidates, we perform a kinematic fit for each B candidate, fixing its mass and energy to their known values.

We study the dynamics of the three-body decay by

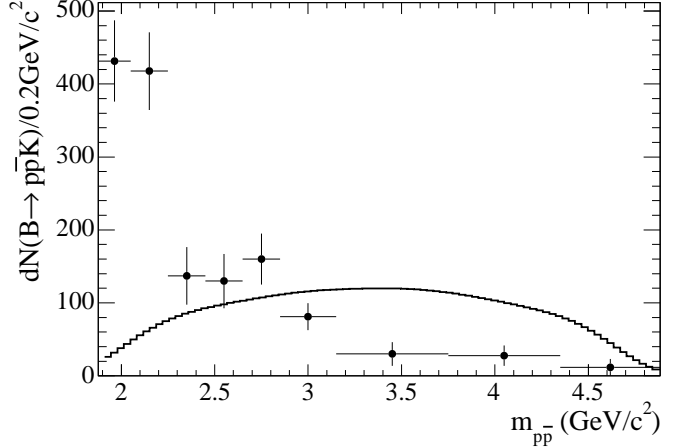


FIG. 4: Efficiency-corrected yield of $B^+ \rightarrow p\bar{p}K^+$ events as a function of $m_{p\bar{p}}$ in data (points) and in three-body phase-space signal MC (histogram). Errors shown are statistical only.

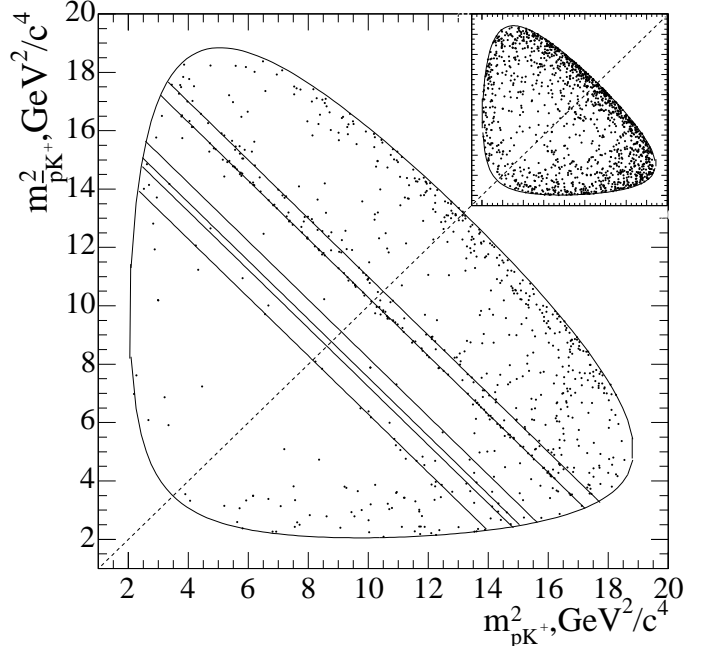


FIG. 5: Dalitz plot of data in the narrow signal region, and sideband region (inset). These distributions are not efficiency-corrected. The lines show the positions of the prominent charmonium backgrounds, from left to right ψ' , $\chi_{c2,1,0}$, J/ψ , η_c . The sideband contains about eight times more combinatorial events than are expected in the signal region.

constructing signal and sideband Dalitz plots (Fig. 5). There are 780 (1661) events in the signal (sideband) region. The sideband contains about eight times more combinatorial events than the signal region. The Dalitz plot for the signal region shows the threshold enhancement in the $p\bar{p}$ mass spectrum, as well as clear diagonal bands corresponding to η_c , J/ψ and ψ' decays.

To study the m_{pK^+} and $m_{\bar{p}K^+}$ asymmetry, we divide the Dalitz plot along the $m_{pK^+} = m_{\bar{p}K^+}$ line (dashed line in Fig. 5) and each of the two halves is projected

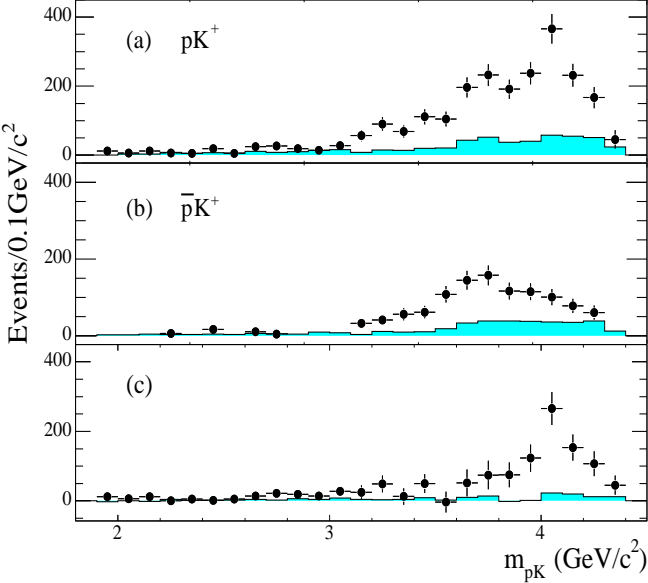


FIG. 6: Efficiency-corrected distributions in the narrow signal (points) and rescaled sideband (shade) regions: (a) m_{pK^+} (for $m_{pK^+} > m_{\bar{p}K^+}$), (b) $m_{\bar{p}K^+}$ (for $m_{pK^+} < m_{\bar{p}K^+}$), and (c) difference between (a) and (b). Errors shown are statistical only.

onto the nearer axis. The corresponding distributions for the events in signal and rescaled sideband regions are shown in Fig. 6(a,b). No asymmetry is expected from variations in $\varepsilon_{m_{p\bar{p}}}$ which is charge-symmetric and slowly varying with $m_{p\bar{p}}$, nor from the small combinatorial background shown in Fig. 6(a,b). The asymmetry appears as a broad enhancement peaking at about 4 GeV in the pK^+ combinations (Fig. 6(c)). This could be an indication of a correlation between quarks in \bar{p} and K^+ if the B decay proceeds through a penguin diagram (Fig. 1(a)). No quantitative theoretical description of this correlation is available at the moment.

The two-body decay $B^+ \rightarrow p\bar{\Lambda}(1520)$ could also be present in the $p\bar{p}K^+$ signal sample. The efficiency for detection of this channel is determined in dedicated MC simulation to be $(4.7 \pm 0.1)\%$, including $\mathcal{B}(\bar{\Lambda}(1520) \rightarrow pK^-)$ [13]. The $m_{\bar{p}K^+}$ spectrum, shown in Fig. 7(a), is fit with an ARGUS function [15] for the background and a Breit-Wigner convolved with a double Gaussian (with a common mean) for the $\bar{\Lambda}(1520)$ signal shape. The mass resolutions and the ratio of areas of the Gaussians are fixed to the values obtained from MC simulation, while we fix the mean and the natural width to established values [13]; the endpoint of the ARGUS function is fixed to the sum of the proton and kaon masses. An unbinned maximum likelihood fit (Fig. 7(a)) results in an upper limit (U.L.) on $\mathcal{B}(B^+ \rightarrow p\bar{\Lambda}(1520))$ of 1.5×10^{-6} at 90% C.L. (including a systematic error of 16%).

The search for a light Θ^{*++} pentaquark candidate ($m_{\Theta^{*++}} < 2 \text{ GeV}/c^2$) [16] proceeds as follows. From $B^+ \rightarrow p\bar{p}K^+$ three-body phase-space MC as well

TABLE I: Systematic uncertainties in percent on the branching fraction measurements and in the values of uncertainties for the symmetry measurements. Values for $m_{p\bar{p}}$ below 2.85 GeV/c^2 are given in brackets.

Type	$p\bar{p}K^+$	$\eta_c K^+$	$p\bar{\Lambda}(1520)$	$\bar{p}\Theta^{*++}$	A_{ch}
<i>B</i> -counting	1.1(1.1)	1.1	1.1	1.1	—
Tracking/PID	3.8(3.8)	3.4	4.2	4.2	0.02
MC Statistics	2.1(2.4)	0.7	1.0	0.5	0.03
B.F. Errors	0.9(—)	—	2.2	—	—
Selection	0.2(—)	0.4	3.9	3.9	—
$\Delta E/\text{Mass}$ Fits	3.6(2.4)	8.9	14.3	—	0.01
Total	5.8(5.2)	13.5	15.6	6.1	0.03

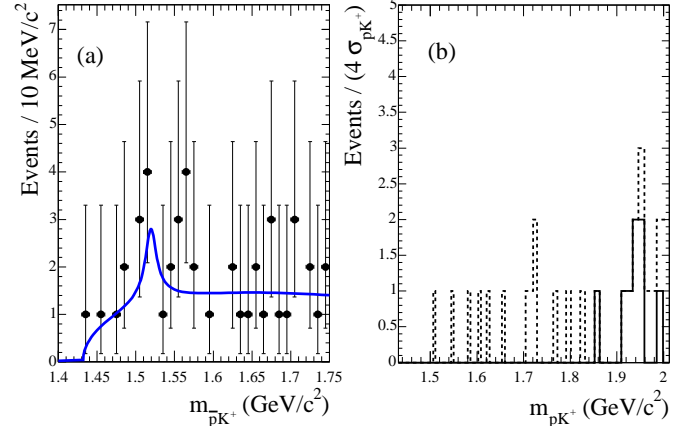


FIG. 7: (a) The $m_{\bar{p}K^+}$ distribution for data events in $\Lambda(1520)$ mass region; (b) The m_{pK^+} distributions for data events in the signal region outside (dashed) or inside (solid) the $2.85 < m_{p\bar{p}} < 3.15 \text{ GeV}/c^2$ region. Distributions are not efficiency corrected.

as five dedicated signal MC samples with $m_{\Theta^{*++}} = 1.5, 1.6, 1.7, 1.8, 1.9 \text{ GeV}/c^2$, we find the mass resolution (σ_{pK^+}) to vary from 1.0 to $3.0 \text{ MeV}/c^2$ for $1.43 < m_{pK^+} < 2.00 \text{ GeV}/c^2$, and the average reconstruction efficiency to be $(20.5 \pm 0.1)\%$ in this mass region. The events with $m_{p\bar{p}}$ in the charmonium region are vetoed. The pK^+ mass distribution of the remaining events is shown in Fig. 7(b). A Bayesian approach is used to calculate the U.L. at 90% C.L. as a function of m_{pK^+} , assuming Poisson-distributed events in the absence of background. Each limit is increased by the total systematic error of 6%. The U.L. for $\mathcal{B}(B^+ \rightarrow \Theta^{*++}\bar{p}) \times \mathcal{B}(\Theta^{*++} \rightarrow pK^+)$ is measured to be 0.5×10^{-7} for $1.43 < m(\Theta^{*++}) < 1.50 \text{ GeV}/c^2$, $< 0.9 \times 10^{-7}$ for $1.50 < m(\Theta^{*++}) < 1.72 \text{ GeV}/c^2$, and $< 1.2 \times 10^{-7}$ for $1.72 < m(\Theta^{*++}) < 2.00 \text{ GeV}/c^2$.

The systematic uncertainties for each analysis are summarized in Table I. The $\Upsilon(4S)$ is assumed to decay equally to $B^0\bar{B}^0$ and $B^+\bar{B}^-$ mesons. Incomplete knowledge of the luminosity and cross-section leads to a 1.1% uncertainty. Charged-tracking and particle-identification (PID) studies in the data lead to small corrections applied to each track in these simulations. Limitation of statistics and purity in these data-MC comparisons lead

to residual tracking/PID uncertainties. A large control sample of $B^+ \rightarrow J/\psi(e^+e^-)K^+$ is separately studied in data and MC simulations to understand the residual errors from the event-shape, ΔE , and m_{ES} cuts. Limitation of MC statistics employed in each analysis contributes to a small uncertainty. Branching fraction uncertainties (B.F. Errors) [13] on $\mathcal{B}(B^+ \rightarrow XK^+) \times \mathcal{B}(X \rightarrow p\bar{p})$, where $X = \chi_{c[0,1,2]}, \psi'$ and $\mathcal{B}(\Lambda(1520) \rightarrow pK^-)$ affect the total $p\bar{p}K^+$ and the $p\bar{\Lambda}$ branching fraction measurements, respectively. Where the MC values are used to fix signal shape parameters in a fit, the parameters are varied within their uncertainties and the data are refit to propagate this uncertainty. In a similar fashion, different ranges and background functions are employed to establish the uncertainty on the mass spectra fits (resulting, for example, in the $\Gamma(\eta_c)$ uncertainty of 3 MeV).

In summary, with 210 fb^{-1} of data, we isolate the $B^+ \rightarrow p\bar{p}K^+$ final state, and measure its non-charmonium branching fraction to be $(5.3 \pm 0.4 \pm 0.3) \times 10^{-6}$ for $m_{p\bar{p}}$ below $2.85\text{ GeV}/c^2$ and $(6.7 \pm 0.5 \pm 0.4) \times 10^{-6}$ for the whole $m_{p\bar{p}}$ range. We measure $A_{ch} = -0.16^{+0.07}_{-0.08} \pm 0.04$ for $m_{p\bar{p}}$ below $2.85\text{ GeV}/c^2$. The existence of a low-mass enhancement of the $p\bar{p}$ pair is confirmed. The asymmetry between pK^+ and $\bar{p}K^+$ final states in the Dalitz plot is demonstrated, providing evidence supporting the dominance of the penguin amplitude in this B decay. We measure the total width of η_c to be $25^{+6}_{-5} \pm 3\text{ MeV}/c^2$. An upper limit of the decay rate to $p\bar{\Lambda}(1520)$ is set at 1.5×10^{-6} . No evidence is found for the pentaquark candidate Θ^{*++} in the mass range 1.43 to $2.0\text{ GeV}/c^2$, decaying into pK^+ , and branching fraction limits are established at the 10^{-7} level.

We thank S.J. Brodsky for useful discussions. The collaboration is grateful for the excellent luminosity and machine conditions provided by our PEP-II colleagues, and for the substantial dedicated effort from the computing organizations that support *BABAR*. The collaborating institutions wish to thank SLAC for its support and kind hospitality. This work is supported by DOE and NSF (USA), NSERC (Canada), IHEP (China), CEA and CNRS-IN2P3 (France), BMBF and DFG (Germany), INFN (Italy), FOM (The Netherlands), NFR (Norway), MIST (Russia), and PPARC (United Kingdom). Indi-

viduals have received support from CONACyT (Mexico), A. P. Sloan Foundation, Research Corporation, and Alexander von Humboldt Foundation.

* Also with Università di Perugia, Dipartimento di Fisica, Perugia, Italy

† Also with Università della Basilicata, Potenza, Italy

‡ Deceased

- [1] Charge-conjugate reactions are included implicitly throughout the paper.
- [2] Belle Collaboration, M.Z. Wang *et al.*, Phys. Rev. Lett. **92**, 131801 (2004).
- [3] C.K. Chua, W.S. Hou, S.Y. Tsai, Phys. Lett. B **544**, 139 (2002).
- [4] J.L. Rosner, Phys. Rev. D **69**, 094014 (2004).
- [5] Belle Collaboration, M.Z. Wang *et al.*, Phys. Rev. Lett. **90**, 201802 (2003); Belle Collaboration, Y.J. Lee *et al.*, Phys. Rev. Lett. **93**, 211801 (2004); CLEO Collaboration, S. Anderson *et al.*, Phys. Rev. Lett. **86**, 2732 (2001).
- [6] BES Collaboration, J.Z. Bai *et al.*, Phys. Rev. Lett. **91**, 022001 (2003).
- [7] C.K. Chua, W.S. Hou, S.Y. Tsai, Phys. Rev. D **66**, 054004 (2002); B. Kerbikov, A. Stavinsky, V. Fedotov, Phys. Rev. C **69**, 055205 (2004).
- [8] H.Y. Cheng, K.C. Yang, Phys. Rev. D **66**, 014020 (2002).
- [9] J.L. Rosner, Phys. Rev. D **68**, 014004 (2003).
- [10] J. Ellis, M. Karliner, M. Praszalowicz, JHEP **0405**, 002 (2004); B. Wu, B.Q. Ma, Phys. Rev. D **69**, 077501 (2004); H. Walliser, V.B. Kopeliovich, J. Exp. Theor. Phys. **97**, 433 (2003); D. Borisyuk, M. Faber, A. Kobushkin, Ukr. J. Phys. **49**, 944 (2004).
- [11] *BABAR* Collaboration, B. Aubert *et al.*, Nucl. Instrum. Methods Phys. Res. A **479**, 1 (2002).
- [12] R.A. Fisher, Ann. Eugenics **7**, 179 (1936).
- [13] Particle Data Group, S. Eidelman *et al.*, Phys. Lett. B, **592**, 1 (2004).
- [14] The *BABAR* detector Monte Carlo simulation is based on GEANT4: S. Agostinelli *et al.*, Nucl. Instrum. Methods Phys. Res. A **506**, 250 (2003).
- [15] ARGUS Collaboration, H. Albrecht *et al.*, Phys. Lett. B **241**, 278 (1990).
- [16] The Θ^{*++} width is assumed to be negligible compared to pK^+ mass resolution.